Hindawi Publishing Corporation
Journal of Biomedicine and Biotechnology
Volume 2010, Article ID 123460, 11 pages
doi:10.1155/2010/123460

Methodology Report

Top-Down Proteomic Identification of Furin-Cleaved α-Subunit of Shiga Toxin 2 from *Escherichia coli* O157:H7 Using MALDI-TOF-TOF-MS/MS

Clifton K. Fagerquist and Omar Sultan

U.S. Department of Agriculture, Western Regional Research Center, Agricultural Research Service, 800 Buchanan Street, Albany, CA 94710, USA

Correspondence should be addressed to Clifton K. Fagerquist, clifton.fagerquist@ars.usda.gov

Received 16 September 2010; Accepted 17 December 2010

Academic Editor: Francesca Cutruzzolà

A method has been developed to identify the α-subunit of Shiga toxin 2 (α-Stx2) from *Escherichia coli* O157:H7 using matrix-assisted laser desorption/ionization time-of-flight-time-of-flight tandem mass spectrometry (MALDI-TOF-TOF-MS/MS) and top-down proteomics using web-based software developed in-house. Expression of Stx2 was induced by culturing *E. coli* O157:H7 on solid agar supplemented with an antibiotic that elicits the bacterial SOS-response. Bacterial cell lysates were incubated in the presence of furin, a human enzyme, that cleaves α-Stx2 into A1 (~28 kDa) and A2 (~5 kDa) protein fragments. A subsequent disulfide reduction step unlinked A1 from A2. MALDI-TOF-MS of the furin-digested/disulfide-reduced sample showed a peak at mass-to-charge (m/z) 5286 that corresponded to the A2 fragment. No peak was observed that corresponded to the A1 fragment although its presence was confirmed by bottom-up proteomics. The peak at m/z 5286 was definitively identified by MALDI-TOF-TOF-MS/MS and top-down proteomics as the A2 fragment of α-Stx2.

1. Introduction

Protein toxins are a major etiological agent of severe illness caused by foodborne bacterial pathogens [1]. The importance of bacterial protein toxins has resulted in the development of techniques to identify them as well as other virulence factors a microorganism may harbor. For example, polymerase chain reaction (PCR) may be used to amplify short segments of toxin genes demonstrating the presence of such genes and the potential of the microorganism to express the toxin [2–4]. Alternatively, an enzyme immunoassay (EIA) may be used to indirectly detect the actual expression of a protein toxin by a microorganism [2, 5, 6]. Another approach for toxin detection is to measure its toxic effects on mammalian cells *in vitro* [7]. Because of its speed, sensitivity, and high specificity, mass spectrometry has been used to unambiguously detect, characterize, and identify chemical compounds including protein toxins [8].

One of the most important bacterial protein toxins is Shiga toxin (also referred to as Shiga-like toxin or verotoxin) [9–11]. Shiga toxin (Stx) is an AB_5 toxin possessing an α- and β-subunit. Five identical β-subunits form a noncovalently assembled donut-shaped complex. A single α-subunit is positioned primarily on one side of the β-complex (A1) and the central core formed from the β-pentamer (A2). A highly accessible 20-residue loop in the polypeptide chain of the α-subunit facilitates cleavage of the α-subunit into its A1 and A2 fragments. The base of the 20-residue loop is linked by a disulfide bond. When released by bacterial cell lysis in the human gut, the holotoxin attaches itself to the glycosphingolipid globotriaosylceramide (Gb3 also referred to as CD^{77}) receptors on the surface of intestinal endothelial cells and/or other cells in the human body that have the same surface receptor, for example, kidney cells [12, 13]. Attachment of the β-complex to Gb3 occurs on the side opposite to that of the α-subunit [9].

The toxin is introduced into eukaryotic cells by endocytosis. Early endosomes are transported, in a retrograde fashion, to the Golgi apparatus and eventually to the endoplasmic reticulum (ER) [9]. At some point in the early

endosome, the α-subunit is proteolytically cleaved by furin, a membrane protein. However, even after this cleavage, the A1 and A2 fragments are still bound by a disulfide bond. This disulfide bond is subsequently reduced in the lumen of the ER, and the catalytically active A1 fragment is then translocated to the cytosol where it disrupts eukaryotic ribosomal protein synthesis eventually resulting in cell death [9, 14].

Previous approaches that use matrix-assisted laser desorption/ionization time-of-flight mass spectrometry (MALDI-TOF-MS) for bacterial identification typically attempt to detect as many bacterial proteins as possible in order to obtain as unique an MS "fingerprint" as possible [15–29]. Alternatively, matrix-assisted laser desorption/ionization time-of-flight time-of-flight tandem mass spectrometry (MALDI-TOF-TOF-MS/MS) has been used to fragment intact bacterial proteins by MS/MS and identify them (and their source microorganism) by top-down proteomic analysis [30–33]. We have recently reported using MALDI-TOF-TOF-MS/MS to ionize, isolate, and fragment intact protein ions from bacterial cell lysates [31, 32]. Using software developed in-house, the mass-to-charge (m/z) of MS/MS fragment ions are compared to a database of *in silico* fragment ion m/z derived from bacterial protein sequences having the same molecular weight (MW) as that of the protein ion. A simple peak matching algorithm [31, 32] and a P-value scoring algorithm (developed by others [30]) were used to independently score/rank identifications. This approach to bacterial protein identification is particularly attractive as sample preparation is simple and does not require pre-enrichment or chromatographic separation of proteins. MALDI-TOF-TOF-MS/MS analysis is quickly accomplished after an equally rapid MALDI-TOF-MS analysis. Both MALDI-TOF-MS and MALDI-TOF-TOF-MS/MS approaches are accomplished by culturing bacterial cells on media that facilitates bacterial growth. However, such growth conditions do not necessarily result in expression of important bacterial virulence factors which could be used to characterize the pathogenicity of the microorganism.

In the current study, we induce expression of a specific bacterial virulence factor most often linked to cases of severe foodborne illness [12, 13]. We have applied our top-down MALDI-TOF-TOF-MS/MS technique to the identification of the α-subunit of Shiga toxin 2 (α-Stx2) from a genomically sequenced strain of *E. coli* O157:H7 [34]. Expression of α-Stx2 was induced by culturing on a conventional solid agar supplemented with an antibiotic that is a powerful inducer of the bacterial SOS-response [35–38].

2. Material and Methods

2.1. Induction of Stx2 from E. coli O157:H7. The *E. coli* O157:H7 strain used in the current study is the genomically sequenced strain EDL933 (ATCC # 43895) which possesses the gene for Shiga toxin 2 (stx_2) as well as other virulence factors [34]. Expression of Stx2 in *E. coli* O157:H7 was induced by overnight culturing at 37°C on Luria-Bertani agar (LBA) plates supplemented with 20 ng/mL of ciprofloxacin (CP), a fluoroquinolone antibiotic. The use of fluoroquinolones to induce expression of Stx has been described previously [35–38].

2.2. In Vitro Furin-Induced Cleavage of α-Stx2. One μL of bacterial cells was harvested with a sterile 1 μL transfer loop and transferred to a sterile 2 mL microcentrifuge tube containing 300 μL of a sterile solution of 3 mM molecular grade $CaCl_2$ (Sigma-Aldrich, St. Louis, MO) in HPLC grade water (Burdick and Jackson) and approximately 100 mg of 0.1 mm zirconia-silica beads (BioSpec Products, Bartlesville, OK). The tubes were bead-beat for 60 seconds on a reciprocating shaker (Mini-Beadbeater; Biospec Products, Bartlesville, OK) after which they were centrifuged at 14,000 rpm for 2 minutes.

One μL of furin enzyme (2000 units/mL, New England BioLabs, Ipswich, MA) was added to 30 μL of bacterial cell supernatant in a sterile 500 μL thin-walled PCR tube and incubated at 37°C for 10, 30, or 60 minutes. The furin recognition site (RXXR) for cleavage of the α-Stx2 is located in a highly accessible loop of the polypeptide chain between two cysteine residues (Cys^{241} and Cys^{260}) which form an intramolecular disulfide bond (Figure 1) [14, 39]. After furin digestion, 1.5 μL of 1 M molecular grade dithiothreitol (DTT, Sigma-Aldrich, St. Louis, MO) was added to the reaction mixture followed by incubation at 70°C for 10 minutes in order to reduce the intramolecular disulfide bond and unlink the two fragments (A1 and A2) of the α-subunit. DTT appeared to inhibit furin enzyme activity; in consequence, it was added *after* completion of the furin digestion step. A negative control in the absence of furin and DTT was also performed. The reaction products were analyzed by MS and MS/MS.

2.3. One-Dimensional Polyacrylamide Gel Electrophoresis (1D PAGE). Approximately, 2 μL of bacterial cells were harvested from a CP-supplemented LBA solid agar plate after overnight growth and transferred to a microcentrifuge tube with 300 μL of extraction solution and processed as previously described. For one sample, 4 μL of furin were added to 30 μL of bacterial cell lysate and incubated at 37°C for 3 hours followed by a disulfide reduction step as previously described. A 19.5 μL aliquot of this sample was combined with 6.5 μL of NuPAGE LDS Sample Buffer (Invitrogen, Carlsbad, CA). For another sample, 16.9 μL of bacterial cell lysate was added to 6.5 μL LDS sample buffer and 2.6 μL NuPAGE reducing agent (NuPAGE, Invitrogen, Carlsbad, CA) and incubated for 10 minutes at 70°C. A total of 25 μL of each sample was applied to separate lanes of a 1.0 mm NuPAGE Novex 4–12% Bis-Tris mini-gel (NuPAGE, Invitrogen, Carlsbad, CA). The upper (cathode) buffer chamber consisted of 200 mL of MES SDS running buffer containing 500 μL of NuPAGE antioxidant reagent (Invitrogen, Carlsbad, CA) to maintain proteins in a reduced state during electrophoresis. A constant-voltage (200 V) was applied for 40 minutes. The gel was stained with a Coomasie staining solution (SimplyBlue-SafeStain, Invitrogen, Carlsbad, CA) using the supplier's microwave procedure and imaged (Supplementary Materials). Relevant gel bands were excised and in-gel digested with porcine

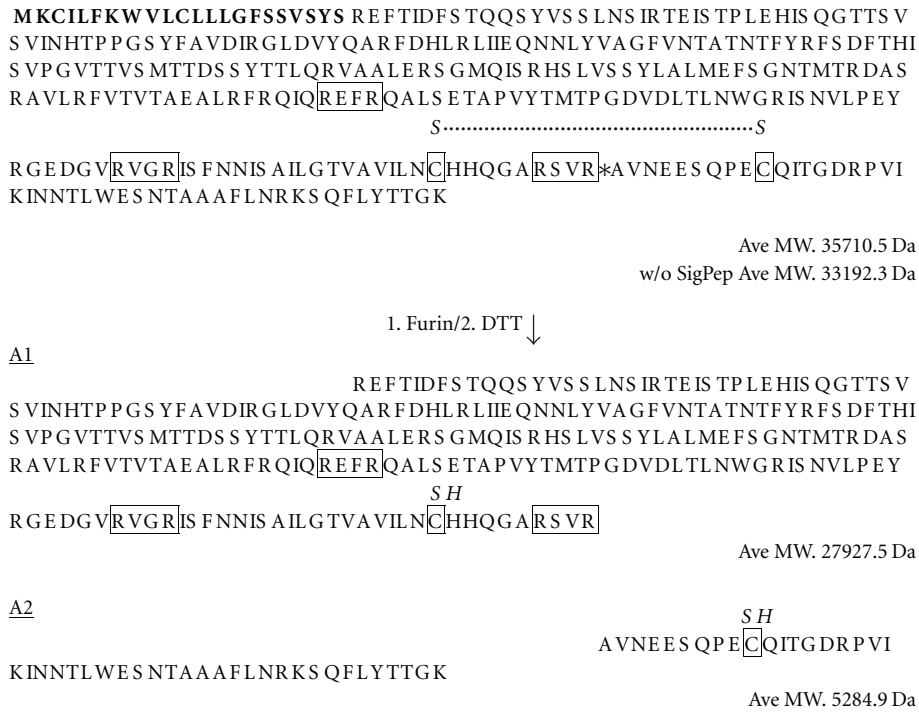

Figure 1: Sequence of α-Stx2 from *E. coli* O157:H7 (EDL933). A 22-residue signal peptide (in bold) is removed in the mature protein, and cysteines involved in an intramolecular disulfide bond ($S \cdots S$) are boxed. Potential furin cleavage recognition sites (RXXR) are boxed. An asterisk ($*$) marks the observed furin cleavage site. In eukaryotic cells, after disulfide reduction, the catalytically active α_{A1}-Stx2 fragment is translocated to the cytosol and the α_{A2}-Stx2 fragment remains associated with the β-pentamer.

trypsin (Promega, Madison, WI) using standard protocols (DigestPro, Intavis, Langenfeld, Germany).

2.4. Bottom-Up Proteomic Analysis. Twenty μL of each digest were separated by nano-HPLC (LC Packings/Dionex, Sunnyvale, CA) and analyzed by MS and MS/MS using a Q-Star-Pulsar I (Applied Biosytems, Foster City, CA) [40]. Peptides (and their corresponding proteins) were identified by analysis of MS and MS/MS data using MASCOT [41] using NCBInr and SwissProt databases. Taxonomy was left unrestricted so as to search against both bacterial and bacteriophage databases. The top protein/organism identifications were *Escherichia coli* and/or enterobacteria phage BP-933W which is present in the *E. coli* O157:H7 (strain EDL933). Peptide and protein identifications are provided in Supplementary Materials available online at doi: 10.1155/2010/123460.

2.5. MALDI-TOF-MS and MS/MS. Mass spectrometry and top-down analysis has been described in detail [31, 32]. Briefly, 0.5 μL of sample was spotted onto a 384-well stainless steel target and allowed to dry at room temperature. The dried sample spot was overlayed with 0.5 μL aliquot of saturated MALDI matrix solution of α-cyano-4-hydroxycinnamic acid (HCCA, Fluka Analytical) or 3,5-dimethoxy-4-hydroxycinnamic acid (sinapinic acid, Fluka Analytical) in 67% HPLC grade water, 33% HPLC grade acetonitrile, and 0.2% trifluoroacetic acid. MS and MS/MS analysis was performed using a 4800 Plus MALDI-TOF/TOF tandem mass spectrometer (Applied Biosystems, Foster City, CA) equipped with a 200 Hz YAG laser (λ = 355 nm).

MS analysis was performed in linear positive ion mode using default instrument settings. Ions were accelerated from the first source at 20 kV. The linear mode was externally calibrated with a mixture of cytochrome C (MW = 12,361.088 Da), lysozyme (MW = 14,306.200 Da), and myoglobin (MW = 16,952.551 Da). MS spectra were acquired using 1000 laser shots. MS/MS analysis was performed in positive ion reflectron mode. The reflectron mode was externally calibrated using the fragment ions at mass-to-charge (m/z) of 175.119, 684.346, 813.389, 1,056.475, and 1,441.634 from postsource dissociation (PSD) of the singly charged (protonated) precursor ion of glu-fibrino-peptide B (Sigma-Aldrich, MW = 1,570.60 Da).

For intact protein ion fragmentation, the instrument was operated using the default settings of the operating mode: MS/MS 1 kV positive sensitivity. The metastable suppressor was enabled and the timed ion selector (TIS) was operated at a resolution of $\pm$100 Da. In order to maximize protein ion fragmentation efficiency, a higher than normal laser fluence was utilized [30–32]. Positive ions were accelerated from the source at 8.0 kV, decelerated to 1 kV in the collision cell, and reaccelerated to 15 kV in the second source. However, no target gas was introduced into the collision cell. MS/MS data were acquired using 10,000 laser shots.

Raw MS and MS/MS data were processed using the commercial software provided with the instrument (Data

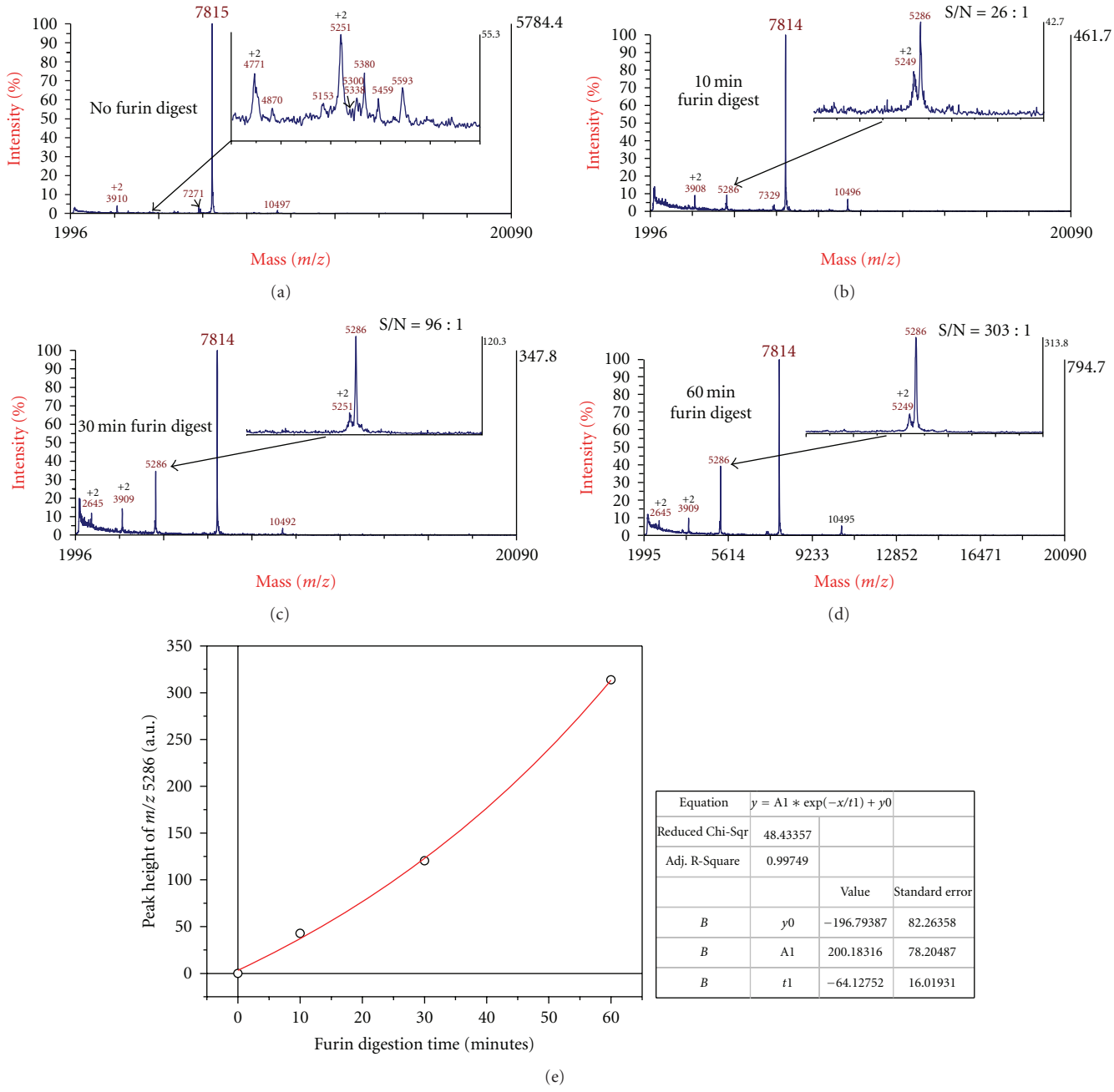

FIGURE 2: MALDI-TOF-MS of bacterial cell lysates at different furin digestion times. Bottom panel is a plot of peak height of *m/z* 5286 versus furin digestion time. Data points are fitted to a simple exponential function.

Explorer v4.9, Applied Biosystems, Foster City, CA). MS spectra were processed with a noise filter (correlation factor = 0.7) and then centroided. MS/MS spectra were processed, first with an advanced baseline correction (peak width = 32, flexibility = 0.5, degree = 0.1), followed by a noise removal (standard deviation = 2), followed by a Gaussian smooth (filter width = 31 points), and then centroided. Processed MS and MS/MS data were exported from the instrument software as an ASCII file (*m/z* versus absolute intensity) and then uploaded to their respective databases in the USDA software.

2.6. Top-Down Proteomic Analysis. The USDA software and its use for top-down proteomic analysis has been described in detail [32]. Briefly, the program rapidly compares the *m/z* of MS/MS fragments to the *m/z* of *in silico* fragment ions derived from bacterial protein sequences that have the same molecular weight (MW) as that of the protein biomarker ion being analyzed. The program was written using a Java runtime environment with MySQL database management and a Tomcat/Apache web interface. Bacterial protein sequences were retrieved using the *TagIdent* software tool from *ExPASy* website (http://www.expasy.org/) from

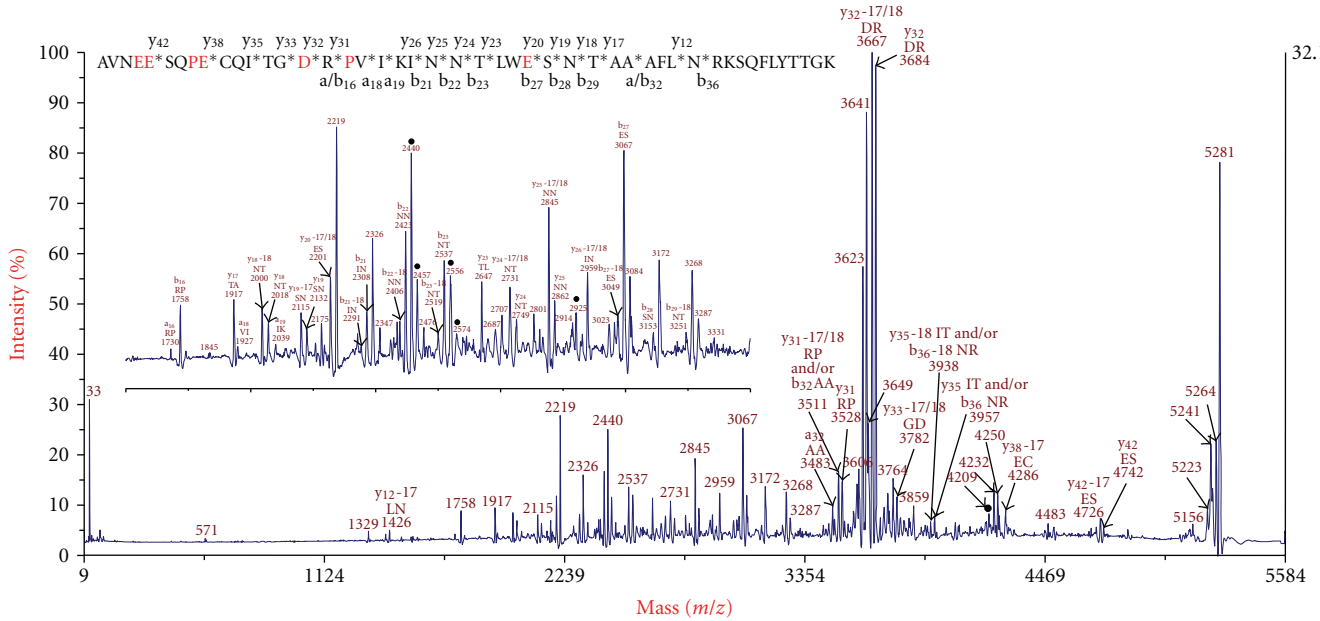

Figure 3: MS/MS of the precursor ion at m/z 5286 in Figure 2. Fragment ions marked with a solid circle were also observed in the MS/MS spectrum of the precursor ion at m/z 5250 (Figure S1). Fragment ions matched to *in silico* fragments ions of α_{A2}-Stx2 are identified by their ion type/number and the two amino acid residues adjacent to the site of polypeptide cleavage. Sequence of α_{A2}-Stx2. Asterisk indicates site of gas phase fragmentation with corresponding ion type/number. D, E, and P residues are highlighted in red.

UniProtKB/Swiss-Prot databases (versions 18-May-2010 or 15-June-2010). The downloaded multisequence FASTA files were processed using a beta-version GPMAW (version 8.01 a5) and the resulting files were uploaded to the *in silico* database of the USDA software. The USDA software uses a simple peak matching algorithm [32] and a *P*-value algorithm (developed by Demirev and coworkers [30]) to independently score/rank MS/MS-to-*in silico* comparisons.

3. Results and Discussion

Figure 1 shows the full protein sequence of the α-Stx2 from *E. coli* O157:H7 strain EDL933 (ave. MW = 35,710.5 Da). However, this protein toxin has a 22-residue N-terminal signal peptide as well as a disulfide bridge between Cys^{263} and Cys^{282} (Cys^{241} and Cys^{260} in the posttranslationally modified protein). The posttranslationally modified MW of α-Stx2 is thus 33,192.3 Da. Furin cleavage of the α-Stx2 (followed by disulfide reduction) should result in formation of two fragments: A1 (α_{A1}-Stx2) with an average MW of 27,927.5 Da and A2 (α_{A2}-Stx2) with an average MW of 5284.9 Da. Figure 2 shows MALDI-TOF-MS spectra of furin-digested bacterial cell lysate of *E. coli* O157:H7 cultured on solid agar supplemented with 20 ng/mL of ciprofloxacin. Furin digestion times are indicated for each MALDI-TOF-MS spectrum. Each spectrum includes an insert of the expanded display range at ~m/z 5300. The most prominent peak in the spectra in Figure 2 is at ~m/z 7814. This protein ion peak corresponds to the β-subunit of Stx2 (β-Stx2) as identified by top-down proteomic analysis [42]. As each β-subunit monomer is part of a pentamer complex in solution to which a single α-subunit is associated, it is to be expected that the β-subunit is the most prominent protein ion given the 1 : 5 stoichiometric ratio of $\alpha : \beta$ subunits for the AB_5 holotoxin [9]. A peak at m/z ~ 5286, corresponding to the α_{A2}-Stx2, is not observed when furin digestion is not included in the sample preparation (Figure 2(a)). A peak observed at m/z 5251 is approximately one-half the m/z of a peak at m/z 10497. MS/MS of the peaks at m/z 5251 and m/z 10497 was performed which showed several prominent fragment ions that were common to both MS/MS spectra suggesting that these ions are the +2 and +1 charge state of the same protein, respectively (Supplementary Materials). Unfortunately, we were unable to identify this protein by either top-down or bottom-up proteomic analysis. The data acquisition upper mass range was extended up to m/z 30,000; however, no peaks were observed that corresponded to α_{A1}-Stx2.

Furin digestion of the bacterial cell lysate for 10 minutes resulted in the MALDI-TOF-MS spectrum (Figure 2(b)) which shows the sudden appearance of what is presumably a singly charged ion at m/z 5286. The neighboring doubly charged ion at m/z ~ 5250 is also present. As the furin digestion time increases from 10 to 30 to 60 minutes, the absolute intensity of the peak at m/z 5286 increases proportionally with a concomitant increase in its signal-to-noise (S/N). A plot of the absolute intensity of the peak at m/z 5286 as a function of furin digestion time is shown in Figure 2(e). Data points were fitted to a simple exponential. The strong correlation between peak intensity and furin digestion time suggests that the peak at m/z 5286 is the α_{A2}-Stx2. In order to definitively identify it, this peak was subjected to MALDI-TOF-TOF-MS/MS and top-down analysis.

Figure 3 shows the MS/MS spectrum of the peak at *m/z* 5286. Prominent MS/MS fragment ions are identified by their *m/z*. Fragment ions with a corresponding *in silico* fragment ion match to the top-ranked protein identification (α_{A2}-Stx2 in Table 1) are identified by their *m/z*, the *in silico* fragment ion type/number and the two amino acid residues immediately adjacent to the sequence cleavage site that resulted in the fragment ion. Some of the more intense MS/MS fragment ions are matched to *in silico* fragment ions adjacent to aspartic acid (D), glutamic acid (E), and proline (P) residues. Fragmentation of the polypeptide chain of singly charged (protonated) protein ions at D, E, or P residues has been noted previously [30–33, 43]. These residues facilitate fragmentation by either transferring a proton from their side-chain to the polypeptide backbone (as in the case of D and E residues) or by creating an internal energy bottleneck in the molecule (as in the case of P residue that results in a 90° turn in the polypeptide backbone). As shown in Figure 3, a number of MS/MS fragment ions were also matched to *in silico* fragment ions that are adjacent to non-D/E/P-residues. The relatively small size of this protein ion results in fragmentation throughout the entire polypeptide as shown in the insert of Figure 3 (not just at D, E, or P residues). The fragmentation efficiency of smaller protein ions is higher compared to larger protein ions due to the fact that larger protein ions have a greater number of vibrational degrees-of-freedom to redistribute their internal energy. In the current experiment, energy is deposited into the protein during laser desorption/ionization. The energy is then rapidly redistributed and the metastable protein ion fragments sometime after exiting the source, that is, postsource dissociation or PSD. As the size of the protein ion being analyzed increases, fragmentation is more likely to occur at dissociation channels that require the least amount of energy, that is, cleavage at D, E, or P residues.

Six prominent fragment ion peaks in Figure 3 (marked by solid circle) had no corresponding *in silico* match to the α_{A2}-Stx2 sequence but were found to be present in the MS/MS spectrum of the doubly charged ion at $m/z \sim 5250$ (Figure S1, Supplementary Materials). Even at the highest TIS resolution (±50 Da), it was not possible to fully resolve and thus mass isolate the ion at *m/z* 5286 from the ion at $m/z \sim 5251$. In consequence, some fragment ions from the precursor ion at *m/z* 5251 are present in the MS/MS spectrum for *m/z* 5286.

Table 1 shows the top ranked identifications of the protein ion at *m/z* 5286 analyzed by MALDI-TOF-TOF-MS/MS and top down proteomics. MS/MS fragment ions were analyzed using a non-residue-specific *in silico* comparison to 3833 bacterial protein sequences having the same MW as that of the biomarker (within ±10 Da). The top-ranked identification of both the USDA score and the *P*-value is the A2 fragment of the furin-cleaved α-Stx2. Nearly all of the more prominent MS/MS fragment ions shown in Figure 3 were matched to *in silico* fragment ions of α_{A2}-Stx2. The theoretical and observed MW also corresponded excellently. As can be seen from Table 1, the sequence of α_{A2}-Stx2 is common to several serotypes and strains of *E. coli* (including O157:H7) as well as *Acinetobacter haemolyticus* and many bacteriophages. Bacteriophages play a critical rôle in facilitating horizontal gene transfer across bacterial genera, species, subspecies, subtypes, and strains [44, 45]. The fact that *A. haemolyticus* has recently been reported to carry the Stx2 gene [46] suggests that the spread of Stx genes (and other virulence factors) across bacteria, facilitated by bacteriophages, may be increasing. The second ranked identifications in Table 1 have *P*-values that are 10 orders-of-magnitude less significant compared to that of the top-ranked identification. The % of matched MS/MS fragment ions (USDA score) is nearly double that for the top ranked identification compared to second-ranked identifications. The USDA algorithm is approximately 8 times faster (84 seconds) to score than the more mathematically complex *P*-value algorithm (654 seconds) due to the number of MS/MS fragment ions being compared (118) and the number of bacterial protein sequences being compared against (3833).

The A1 fragment of the furin-cleaved α-Stx2 was not observed by MALDI-TOF-MS. In consequence, we analyzed, by 1-D PAGE, the proteins from CP-supplemented and CP-supplemented/furin-digested bacterial cell lysates (Figure S3, Supplementary Materials). In the bacterial cell lysate of the CP-supplemented sample, we observe a band at ~33 kDa which is absent from the CP-supplemented/furin-digested sample. This gel band was excised, in-gel digested, and analyzed by bottom-up proteomics. The band corresponded to α-Stx2 and, as shown in Figure 4, the sequence coverage included partial sequences A1 and A2 and no sequence coverage of the signal peptide as one would expect for the mature protein. The 33 kDa also corresponds closely to the theoretical MW of 33,192.3 Da. In the bacterial cell lysate of the CP-supplemented/furin-digested sample, we observe bands at ~28 kDa and ~5-6 kDa which are absent from the CP-supplemented sample. These bands were also analyzed by bottom-up proteomics and identified as α-Stx2 with partial sequence coverage that was consistent with the A1 and A2 fragments, respectively (Figure 4). These results strongly suggest that both A1 and A2 fragments of α-Stx2 are present in the CP-supplemented/furin-digested sample, but only the A2 fragment is successfully ionized by MALDI.

There are a number of possible explanations that may account for the failure to ionize the A1 fragment of α-Stx2 by MALDI. First, MALDI favors ionization of lower MW proteins and peptides. Second, the primary sequence, secondary, or tertiary structure of A1 may not efficiently ionize (protonate) compared with other analytes present in the sample. We do not observe any evidence for furin cleavage at other potential recognition sites (RXXR) in the primary structure of A1. It is possible these other sites are not readily accessible to furin and may suggest a compact tertiary structure for α_{A1}-Stx2 that thwarts ionization. Third, A1 is the catalytically active fragment that binds to eukaryotic ribosomal RNA and disrupts protein synthesis. It has been previously reported that α_{A1}-Stx2 also binds to prokaryotic RNA or DNA [47]. It is possible that the difficulty in detecting A1 could be due to its being bound to bacterial RNA or DNA whose mass exceeds the upper mass detection limit of our instrument. Preliminary experiments were conducted to process samples with RNAase and DNAase

Table 1: The top identifications of the protein biomarker ion at m/z 5286 analyzed by MALDI-TOF-TOF-MS/MS (Figure 3) and top-down proteomics.

Rank	*In silico* ID	Identifier	Sample name	Protein	USDA score	*P*-value
	86486	>tr|Q7DI68|Q7DI68_ECO57	*Escherichia coli* O157:H7	Shiga toxin 2 α-subunit (furin-cleaved sequence) MW = 5284.9	42.37	2.2$E-$13
	86481	>tr|C6UP09|C6UP09_ECO5T	*Escherichia coli* O157:H7 (strain TW14359/EHEC)	Shiga toxin II α-subunit (furin-cleaved sequence) MW = 5284.9	42.37	2.2$E-$13
	86490	>tr|Q7B5L0|Q7B5L0_ECOLX	*Escherichia coli* O157:Hneg	Shiga toxin 2 α-subunit (furin-cleaved sequence) MW = 5284.9	42.37	2.2$E-$13
	86517	>tr|Q6YII8|Q6YII8_ECOLX	*Escherichia coli* O157:Hneg	Shiga toxin 2 α-subunit (furin-cleaved sequence) MW = 5284.9	42.37	2.2$E-$13
	86463	>tr|B3VKH7|B3VKH7_ECOLX	*Escherichia coli*	Shiga toxin 2 α-subunit (furin-cleaved sequence) MW = 5284.9	42.37	2.2$E-$13
	86464	>tr|C5J4Y3|C5J4Y3_ECOLX	*Escherichia coli*	Shiga toxin 2 α-subunit (furin-cleaved sequence) MW = 5284.9	42.37	2.2$E-$13
1	86467	>tr|Q5WPW9|Q5WPW9_ECOLX	*Escherichia coli*	Shiga toxin 2 α-subunit (furin-cleaved sequence) MW = 5284.9	42.37	2.2$E-$13
	86468	>tr|Q8KU16|Q8KU16_ECOLX	*Escherichia coli*	Shiga toxin 2 α-subunit (furin-cleaved sequence) MW = 5284.9	42.37	2.2$E-$13
	86469	>tr|Q8XBV2|Q8XBV2_ECOLX	*Escherichia coli*	Shiga toxin 2 α-subunit (furin-cleaved sequence) MW = 5284.9	42.37	2.2$E-$13
	86473	>tr|B3VKI5|B3VKI5_ECOLX	*Escherichia coli*	Shiga toxin 2 α-subunit (furin-cleaved sequence) MW = 5284.9	42.37	2.2$E-$13
	86474	>tr|B2MW60|B2MW60_ECOLX	*Escherichia coli*	Shiga toxin 2 α-subunit (furin-cleaved sequence) MW = 5284.9	42.37	2.2$E-$13
	86478	>tr|C7FPV8|C7FPV8_ECOLX	*Escherichia coli*	Shiga toxin 2 α-subunit (furin-cleaved sequence) MW = 5284.9	42.37	2.2$E-$13
	86480	>tr|Q47636|Q47636_ECOLX	*Escherichia coli*	Shiga toxin 2 α-subunit (furin-cleaved sequence) MW = 5284.9	42.37	2.2$E-$13
	86472	>tr|Q1ELX7|Q1ELX7_ECOLX	*Escherichia coli* O111:NM	Shiga toxin II α-subunit (furin-cleaved sequence) MW = 5284.9	42.37	2.2$E-$13
	86483	>tr|Q2L9B4|Q2L9B4_ACIHA	*Acinetobacter haemolyticus*	Shiga toxin II α-subunit (furin-cleaved sequence) MW = 5284.9	42.37	2.2$E-$13
	50965	>sp|P09385|STXA_BP933	Enterobacteria phage 933W	Shiga-like toxin 2 α-sub. (furin-cleaved sequence) MW = 5284.9	42.37	2.2$E-$13
	86458	>sp|P09385|STXA_BP933	Enterobacteria phage 933W	Shiga-like toxin 2 α-sub. (furin-cleaved sequence) MW = 5284.9	42.37	2.2$E-$13
	86459	>tr|Q776E1|Q776E1_9CAUD	Stx2 converting phage II	Shiga toxin 2 α-subunit (furin-cleaved sequence) MW = 5284.9	42.37	2.2$E-$13

Table 1: Continued.

Rank	*In silico* ID	Identifier	Sample name	Protein	USDA score	*P*-value
	86491	>tr|Q776Q3|Q776Q3_BPVT2	Enterobacteria phage VT2-Sa	Shiga-like toxin 2 α-sub. (furin-cleaved sequence) MW = 5284.9	42.37	$2.2E-13$
	86494	>tr|Q77CH9|Q77CH9_9VIRU	Enterobacteria phage LC159	Shiga-like toxin 2 α-sub. (furin-cleaved sequence) MW = 5284.9	42.37	$2.2E-13$
	86499	>tr|Q77CH6|Q77CH6_9VIRU	Enterobacteria phage SC370	Shiga-like toxin 2 α-sub. (furin-cleaved sequence) MW = 5284.9	42.37	$2.2E-13$
	86503	>tr|Q6DWK9|Q6DWK9_9VIRU	Enterobacteria phage A397	Shiga-like toxin 2 α-sub. (furin-cleaved sequence) MW = 5284.9	42.37	$2.2E-13$
	86518	>tr|Q08JA4|Q08JA4_9CAUD	Stx2-converting phage 86	Shiga-like toxin 2 α-sub. (furin-cleaved sequence) MW = 5284.9	42.37	$2.2E-13$
	86519	>tr|B0FEE0|B0FEE0_9CAUD	Enterobacteria phage Min27	Shiga-like toxin 2 α-sub. (furin-cleaved sequence) MW = 5284.9	42.37	$2.2E-13$
	86520	>tr|Q776G1|Q776G1_9CAUD	Stx2 converting phage I	Shiga toxin 2 α-sub. (furin-cleaved sequence) MW = 5284.9	42.37	$2.2E-13$
2	66935	>tr|A1AXT4|A1AXT4_RUTMC	*Ruthia magnifica* sub. *Calyptogena magnifica*	50S ribosomal protein L34 PTM-Met MW = 5280.3	24.58	
	79662	>tr|B1C7H9|B1C7H9_9FIRM	*Anaerofustis stercorihominis* DSM 17244	Putative uncharacterized protein MW = 5283.49		$1.2E-3$
2	68014	>tr|A7FRA0|A7FRA0_CLOB1	*Clostridium botulinum* (strain ATCC 19397/Type A)	Bacteriophage prototoxin, streptolysin S family PTM-Met MW = 5284.93	24.58	
3	66935	>tr|A1AXT4|A1AXT4_RUTMC	*Ruthia magnifica* sub. *Calyptogena magnifica*	50S ribosomal protein L34 PTM-Met MW = 5280.3		$1.4E-3$
2	68024	>tr|A7G124|A7G124_CLOBH	*Clostridium botulinum* (strain Hall/ATCC 3502/NCTC 13319/Type A)	Bacteriophage prototoxin, streptolysin S family PTM-Met MW = 5284.93	24.58	
4	76887	>tr|Q73I98|Q73I98_WOLPM	*Wolbachia pipientis* wMel	Putative uncharacterized protein PTM-Met MW = 5285.2		$3.9E-3$
2	68030	>tr|A7GAP1|A7GAP1_CLOBL	*Clostridium botulinum* (strain Langeland/NCTC 10281/Type F)	Bacteriophage prototoxin, streptolysin S family PTM-Met MW = 5284.93	24.58	
5	67756	>tr|A5ZL78|A5ZL78_9BACE	*Bacteroides caccae* ATCC 43185	Putative uncharacterized protein PTM-Met MW = 5278.67		$5.2E-3$
2	69116	>tr|B1IEJ6|B1IEJ6_CLOBK	*Clostridium botulinum* (strain Okra/Type B1)	Bacteriophage prototoxin, streptolysin S family PTM-Met MW = 5284.93	24.58	
5	75125	>tr|D1P267|D1P267_9ENTR	*Providencia rustigianii* DSM 4541	Putative uncharacterized protein PTM-Met MW = 5287.4		$5.2E-3$

Comparison parameters: minimum intensity threshold: 2; fragment ion tolerance in *m/z*: ±1.5; protein mass tolerance: ±10 Da; number of MS/MS above minimum intensity threshold: 118; non-residue-specific *in silico* comparison; 3833 bacterial protein sequences compared. Algorithm computation times: USDA score 84 seconds, *P*-value 654 seconds.

Gel band at ~33 kDa (lane 3, gel band #1)

MKCILFKWVLCLLLGFSSVSYS REFTIDFSTQQSYVSSLNSIRTEISTPLEHISQGTTSV
SVINHTPPGSYFAVDIRGLDVYQARFDHLRLIIEQNNLYVAGFVNTATNTFYRFSDFTHI
SVPGVTTVSMTTDSSYTTLQRVAALERSGMQISRHSLVSSYLALMEFSGNTMTRDAS
RAVLRFVTVTAEALRFRQIQREFRQALSETAPVYTMTPGDVDLTLNWGRISNVLPEY
RGEDGVRVGRISFNNISAILGTVAVILNCHHQGARSVR*AVNEESQPECQITGDRPVIK
INNTLWESNTAAAFLNRKSQFLYTTGK

Gel band at ~28 kDa (lane 4, gel band #3)

MKCILFKWVLCLLLGFSSVSYS REFTIDFSTQQSYVSSLNSIRTEISTPLEHISQGTTSV
SVINHTPPGSYFAVDIRGLDVYQARFDHLRLIIEQNNLYVAGFVNTATNTFYRFSDFTHI
SVPGVTTVSMTTDSSYTTLQRVAALERSGMQISRHSLVSSYLALMEFSGNTMTRDAS
RAVLRFVTVTAEALRFRQIQREFRQALSETAPVYTMTPGDVDLTLNWGRISNVLPEY
RGEDGVRVGRISFNNISAILGTVAVILNCHHQGARSVR*AVNEESQPECQITGDRPVIK
INNTLWESNTAAAFLNRKSQFLYTTGK

Gel band at ~5-6 kDa (lane 4, gel band #9)

MKCILFKWVLCLLLGFSSVSYS REFTIDFSTQQSYVSSLNSIRTEISTPLEHISQGTTSV
SVINHTPPGSYFAVDIRGLDVYQARFDHLRLIIEQNNLYVAGFVNTATNTFYRFSDFTHI
SVPGVTTVSMTTDSSYTTLQRVAALERSGMQISRHSLVSSYLALMEFSGNTMTRDAS
RAVLRFVTVTAEALRFRQIQREFRQALSETAPVYTMTPGDVDLTLNWGRISNVLPEY
RGEDGVRVGRISFNNISAILGTVAVILNCHHQGARSVR*AVNEESQPECQITGDRPVIK
INNTLWESNTAAAFLNRKSQFLYTTGK

Figure 4: Bottom-up proteomic sequence coverage of α-Stx2 (in red) from select gel bands (Figure S3, Supplementary Materials). A 22-residue signal peptide (in bold) is removed in the mature protein. Recognition sites for potential furin cleavage (RXXR) are boxed. An asterisk (*) marks the only observed furin cleavage site.

on the assumption that cleaving the RNA or DNA into smaller units might facilitate ionization of the A1 fragment. However, the A1 fragment was still not detected by MALDI-TOF-MS.

4. Conclusions

We have detected and identified the antibiotic-induced, furin-cleaved α-Stx2 from *E. coli* O157:H7 using MALDI-TOF-TOF-MS/MS and top-down proteomics. Bacterial cell lysates from growth on conventional solid agar supplemented with ciprofloxacin strongly induced expression of Stx2 allowing ionization by MALDI. The human enzyme furin was used to cleave α-Stx2 at the highly accessible polypeptide loop that joins the A1 and A2 fragments of α-Stx2. A further disulfide-reduction step completely unlinked A1 from A2. In the absence of furin digestion and/or disulfide reduction, no peak was observed that corresponded to the A2 fragment suggesting that both steps, performed sequentially, are necessary for successful release of the α_{A2}-Stx2 and its ionization by MALDI. This sequential two-step process follows the model proposed for eukaryotic intracellular processing of α-Stx [9]. The higher MW α_{A1}-Stx2 fragment, although detected and identified by 1-D gel electrophoresis and bottom-up proteomics, did not appear to ionize efficiently by MALDI as an intact protein.

Top-down proteomics utilizing MALDI-TOF-TOF-MS/MS and PSD is a rapid technique for identifying high copy proteins expressed under standard culturing conditions or highly expressed proteins that have been induced to express under specific culturing conditions. Identification of such proteins can assist in the identification or characterization of bacteria and their potential for causing severe illness due to the virulence factors that they can express, for example, protein toxins.

Disclosure

Mention of a brand or firm name does not constitute an endorsement by the U.S. Department of Agriculture over other of a similar nature not mentioned. This article is a US Government work and is in the public domain in the USA.

References

[1] D. C. Pigott, "Foodborne illness," *Emergency Medicine Clinics of North America*, vol. 26, no. 2, pp. 475–497, 2008.

[2] T. E. Grys, L. M. Sloan, J. E. Rosenblatt, and R. Patel, "Rapid and sensitive detection of Shiga toxin-producing Escherichia coli from nonenriched stool specimens by real-time PCR in comparison to enzyme immunoassay and culture," *Journal of Clinical Microbiology*, vol. 47, no. 7, pp. 2008–2012, 2009.

[3] M. J. Hamilton, A. Z. Hadi, J. F. Griffith, S. Ishii, and M. J. Sadowsky, "Large scale analysis of virulence genes in Escherichia coli strains isolated from Avalon Bay, CA," *Water Research*, vol. 44, no. 18, pp. 5463–5473, 2010.

[4] E. B. Hedican, C. Medus, J. M. Besser et al., "Characteristics of O157 versus Non-O157 Shiga toxin-producing escherichia coli infections in minnesota, 2000–2006," *Clinical Infectious Diseases*, vol. 49, no. 3, pp. 358–364, 2009.

[5] P. J. Gavin, L. R. Peterson, A. C. Pasquariello et al., "Evaluation of performance and potential clinical impact of ProSpecT Shiga Toxin Escherichia coli microplate assay for detection of Shiga Toxin-producing E. coli in stool samples," *Journal of Clinical Microbiology*, vol. 42, no. 4, pp. 1652–1656, 2004.

[6] T. D. K. Kumar, R. M. Urs, K. Balakrishna, H. S. Murali, H. V. Batra, and A. S. Bawa, "Monoclonal antibodies against recombinant hemolysin BL complex of Bacillus cereus," *Hybridoma*, vol. 29, no. 1, pp. 67–71, 2010.

[7] B. Quiñones, S. Massey, M. Friedman, M. S. Swimley, and K. Teter, "Novel cell-based method to detect Shiga toxin 2 from escherichia coli O157:H7 and inhibitors of toxin activity," *Applied and Environmental Microbiology*, vol. 75, no. 5, pp. 1410–1416, 2009.

[8] Y. M. Williamson, H. Moura, D. Schieltz et al., "Mass spectrometric analysis of multiple pertussis toxins and toxoids," *Journal of Biomedicine and Biotechnology*, vol. 2010, Article ID 942365, 2010.

[9] L. Johannes and W. Römer, "Shiga toxins from cell biology to biomedical applications," *Nature Reviews Microbiology*, vol. 8, no. 2, pp. 105–116, 2010.

[10] J. Müthing, C. H. Schweppe, H. Karch, and A. W. Friedrich, "Shiga toxins, glycosphingolipid diversity, and endothelial cell injury," *Thrombosis and Haemostasis*, vol. 101, no. 2, pp. 252–264, 2009.

[11] T. Slanec, A. Fruth, K. Creuzburg, and H. Schmidt, "Molecular analysis of virulence profiles and Shiga toxin genes in food-borne Shiga toxin-producing Escherichia coli," *Applied and Environmental Microbiology*, vol. 75, no. 19, pp. 6187–6197, 2009.

[12] H. Uchida, N. Kiyokawa, H. Horie, J. Fujimoto, and T. Takeda, "The detection of Shiga toxins in the kidney of a patient with hemolytic uremic syndrome," *Pediatric Research*, vol. 45, no. 1, pp. 133–137, 1999.

[13] H. Uchida, N. Kiyokawa, T. Taguchi, H. Horie, J. Fujimoto, and T. Takeda, "Shiga toxins induce apoptosis in pulmonary epithelium-derived cells," *Journal of Infectious Diseases*, vol. 180, no. 6, pp. 1902–1911, 1999.

[14] O. Garred, B. van Deurs, and K. Sandvig, "Furin-induced cleavage and activation of Shiga toxin," *Journal of Biological Chemistry*, vol. 270, no. 18, pp. 10817–10821, 1995.

[15] R. J. Arnold and J. P. Reilly, "Fingerprint matching of E. coli strains with matrix-assisted laser desorption/ionization time-of-flight mass spectrometry of whole cells using a modified correlation approach," *Rapid Communications in Mass Spectrometry*, vol. 12, no. 10, pp. 630–636, 1998.

[16] M. A. Claydon, S. N. Davey, V. Edwards-Jones, and D. B. Gordon, "The rapid identification of intact microorganisms using mass spectrometry," *Nature Biotechnology*, vol. 14, no. 11, pp. 1584–1586, 1996.

[17] Y. Dai, L. Li, D. C. Roser, and S. R. Long, "Detection and identification of low-mass peptides and proteins from solvent suspensions of Escherichia coli by high performance liquid chromatography fractionation and matrix-assisted laser desorption/ionization mass spectrometry," *Rapid Communications in Mass Spectrometry*, vol. 13, no. 1, pp. 73–78, 1999.

[18] P. A. Demirev and C. Fenselau, "Mass spectrometry for rapid characterization of microorganisms," *Annual Review of Analytical Chemistry*, vol. 1, no. 1, pp. 71–93, 2008.

[19] C. K. Fagerquist, A. H. Bates, S. Heath et al., "Sub-speciating Campylobacter jejuni by proteomic analysis of its protein biomarkers and their post-translational modifications," *Journal of Proteome Research*, vol. 5, no. 10, pp. 2527–2538, 2006.

[20] C. Fenselau and P. A. Demirev, "Characterization of intact microorganisms by MALDI mass spectrometry," *Mass Spectrometry Reviews*, vol. 20, no. 4, pp. 157–171, 2001.

[21] A. M. Haag, S. N. Taylor, K. H. Johnston, and R. B. Cole, "Rapid identification and speciation of haemophilus bacteria by matrix-assisted laser desorption/ionization time-of-flight mass spectrometry," *Journal of Mass Spectrometry*, vol. 33, no. 8, pp. 750–756, 1998.

[22] R. D. Holland, C. R. Duffy, F. Rafii et al., "Identification of bacterial proteins observed in MALDI TOF mass spectra from whole cells," *Analytical Chemistry*, vol. 71, no. 15, pp. 3226–3230, 1999.

[23] K. H. Jarman, S. T. Cebula, A. J. Saenz et al., "An algorithm for automated bacterial identification using matrix- assisted laser desorption/ionization mass spectrometry," *Analytical Chemistry*, vol. 72, no. 6, pp. 1217–1223, 2000.

[24] T. Krishnamurthy and P. L. Ross, "Rapid identification of bacteria by direct matrix-assisted laser desorption/ionization mass spectrometric analysis of whole cells," *Rapid Communications in Mass Spectrometry*, vol. 10, no. 15, pp. 1992–1996, 1996.

[25] J. O. Lay Jr., "MALDI-TOF mass spectrometry of bacteria," *Mass Spectrometry Reviews*, vol. 20, no. 4, pp. 172–194, 2001.

[26] R. E. Mandrell, L. A. Harden, A. Bates, W. G. Miller, W. F. Haddon, and C. K. Fagerquist, "Speciation of Campylobacter coli, C. jejuni, C. helveticus, C. lari, C. sputorum, and C. upsaliensis by matrix-assisted laser desorption ionization-time of flight mass spectrometry," *Applied and Environmental Microbiology*, vol. 71, no. 10, pp. 6292–6307, 2005.

[27] K. L. Wahl, S. C. Wunschel, K. H. Jarman et al., "Analysis of microbial mixtures by matrix-assisted laser desorption/ionization time-of-flight mass spectrometry," *Analytical Chemistry*, vol. 74, no. 24, pp. 6191–6199, 2002.

[28] Z. Wang, L. Russon, L. Li, D. C. Roser, and S. R. Long, "Investigation of spectral reproducibility in direct analysis of bacteria proteins by matrix-assisted laser desorption/ionization time-of-flight mass spectrometry," *Rapid Communications in Mass Spectrometry*, vol. 12, no. 8, pp. 456–464, 1998.

[29] S. C. Wunschel, K. H. Jarman, C. E. Petersen et al., "Bacterial analysis by MALDI-TOF mass spectrometry: an inter-laboratory comparison," *Journal of the American Society for Mass Spectrometry*, vol. 16, no. 4, pp. 456–462, 2005.

[30] P. A. Demirev, A. B. Feldman, P. Kowalski, and J. S. Lin, "Top-down proteomics for rapid identification of intact microorganisms," *Analytical Chemistry*, vol. 77, no. 22, pp. 7455–7461, 2005.

[31] C. K. Fagerquist, B. R. Garbus, W. G. Miller et al., "Rapid identification of protein biomarkers of escherichia coli O157:H7 by matrix-assisted laser desorption Ionization-time-of-flight-time-of-flight mass spectrometry and top-down proteomics," *Analytical Chemistry*, vol. 82, no. 7, pp. 2717–2725, 2010.

[32] C. K. Fagerquist, B. R. Garbus, K. E. Williams, A. H. Bates, S. Boyle, and L. A. Harden, "Web-based software for rapid top-down proteomic identification of protein biomarkers, with implications for bacterial identification," *Applied and Environmental Microbiology*, vol. 75, no. 13, pp. 4341–4353, 2009.

[33] C. K. Fagerquist, B. R. Garbus, K. E. Williams, A. H. Bates, and L. A. Harden, "Covalent attachment and dissociative

loss of sinapinic acid to/from cysteine-containing proteins from bacterial cell lysates analyzed by MALDI-TOF-TOF mass spectrometry," *Journal of the American Society for Mass Spectrometry*, vol. 21, no. 5, pp. 819–832, 2010.

[34] N. T. Perna, G. Plunkett, V. Burland et al., "Genome sequence of enterohaemorrhagic Escherichia coli O157:H7," *Nature*, vol. 409, no. 6819, pp. 529–533, 2001.

[35] B. Köhler, H. Karch, and H. Schmidt, "Antibacterials that are used as growth promoters in animal husbandry can affect the release of Shiga-toxin-2-converting bacteriophages and Shiga toxin 2 from Escherichia coli strains," *Microbiology*, vol. 146, no. 5, pp. 1085–1090, 2000.

[36] A. Matsushiro, K. Sato, H. Miyamoto, T. Yamamura, and T. Honda, "Induction of prophages of enterohemorrhagic Escherichia coli O157:H7 with norfloxacin," *Journal of Bacteriology*, vol. 181, no. 7, pp. 2257–2260, 1999.

[37] B. Michel, "After 30 years of study, the bacterial SOS response still surprises us," *PLoS Biology*, vol. 3, no. 7, article e255, 2005.

[38] X. Zhang, A. D. McDaniel, L. E. Wolf, G. T. Keusch, M. K. Waldor, and D. W. K. Acheson, "Quinolone antibiotics induce Shiga toxin-encoding bacteriophages, toxin production, and death in mice," *Journal of Infectious Diseases*, vol. 181, no. 2, pp. 664–670, 2000.

[39] A. G. Remacle, S. A. Shiryaev, E. S. Oh et al., "Substrate cleavage analysis of furin and related proprotein convertases: a comparative study," *Journal of Biological Chemistry*, vol. 283, no. 30, pp. 20897–20906, 2008.

[40] C. K. Fagerquist, W. G. Miller, L. A. Harden et al., "Genomic and proteomic identification of a DNA-binding protein used in the "fingerprinting" of Campylobacter species and strains by MALDI-TOF-MS protein biomarker analysis," *Analytical Chemistry*, vol. 77, no. 15, pp. 4897–4907, 2005.

[41] D. N. Perkins, D. J. C. Pappin, D. M. Creasy, and J. S. Cottrell, "Probability-based protein identification by searching sequence databases using mass spectrometry data," *Electrophoresis*, vol. 20, no. 18, pp. 3551–3567, 1999.

[42] C. K. Fagerquist and O. Sultan, "Rapid identification of β-subunit Shiga toxin from Escherichia coli O157:H7 by MALDI-TOF-TOF-MS/MS and top-down proteomics," accepted to *Analyst*.

[43] M. Lin, J. M. Campbell, D. R. Mueller, and U. Wirth, "Intact protein analysis by matrix-assisted laser desorption/ionization tandem time-of-flight mass spectrometry," *Rapid Communications in Mass Spectrometry*, vol. 17, no. 16, pp. 1809–1814, 2003.

[44] B. G. Kelly, A. Vespermann, and D. J. Bolton, "The role of horizontal gene transfer in the evolution of selected foodborne bacterial pathogens," *Food and Chemical Toxicology*, vol. 47, no. 5, pp. 951–968, 2009.

[45] B. G. Kelly, A. Vespermann, and D. J. Bolton, "Horizontal gene transfer of virulence determinants in selected bacterial foodborne pathogens," *Food and Chemical Toxicology*, vol. 47, no. 5, pp. 969–977, 2009.

[46] G. Grotiuz, A. Sirok, P. Gadea, G. Varela, and F. Schelotto, "Shiga toxin 2-producing Acinetobacter haemolyticus associated with a case of bloody diarrhea," *Journal of Clinical Microbiology*, vol. 44, no. 10, pp. 3838–3841, 2006.

[47] J. K. Suh, C. J. Hovde, and J. D. Robertus, "Shiga toxin attacks bacterial ribosomes as effectively as eucaryotic ribosomes," *Biochemistry*, vol. 37, no. 26, pp. 9394–9398, 1998.